dehyde-inhibited signal of xanthine oxidase.

This work demonstrates that the ESR line broadening (or narrowing) mechanism discussed in the context of copper(II) species[9] has considerably wider relevance and provides strong motivation for further examination of other transition metal species in the S-band range of frequencies, For example, ^{77}Se satellites from naturally abundant ^{77}Se (7.58 atom %) in $[Mo(SePh)_4]^-$ are resolved simply by lowering the frequency. Further progress in elucidating details of moderate to weak ligand hyperfine coupling would depend upon availability of techniques such as electron spin echo envelope modulation.[59,60]

(59) Mims, W. B.; Peisach, J. *Biol. Magn. Reson.* **1982**, *3*, 213.
(60) Reijirse, E. J.; van Aerle, N. A. J. M.; Keijzers, C. P.; Bottcher, R.; Kirmse, R.; Stach, J. *J. Mag. Reson.* **1986**, *67*, 114.

Successful computer simulation at more than one frequency is required for unambiguous determination of spin-Hamiltonian and line-width parameters, In the present work, this was achieved for $[Mo(abt)_3]^-$, $[MO(XPh)_4]^-$, and $[MoOL(DMF)]^+$ (L = salen, salophen), but not for $[MoO(qtl)_2Cl]$.

Acknowledgment. J.R.P. and A.G.W. acknowledge support from the Australian Research Grants Scheme. G.R.H. and G.L.W. are grateful for the award of La Trobe and Commonwealth postgraduate scholarships, respectively.

Registry No. ^{17}O, 13968-48-4; ^{77}Se, 14681-72-2; ^{35}C, 13981-72-1; ^{37}Cl, 13981-73-2; $[Mo(abt)_3]^-$, 52820-25-4; $Et_4N[MoO(SPh)_4]$, 65892-35-5; $Et_4N[MoO(SePh)_4]$, 76771-61-4; $Et_4N[WO(SPh)_4]$, 76771-66-9; $Et_4N[WO(SePh)_4]$, 76771-73-8; $[MoO(qtl)_2Cl]$, 23727-65-3; $[MoO(qtl)_Br]$, 89653-39-4; $[MoO(salen)(DMF)]^+$, 107271-65-8; $[MoO(salophen)(DMF)]^+$, 107271-66-9.

Mechanism of the Gauche Conformational Effect in 3-Halogenated 1,5-Benzodioxepins

P. Dionne and M. St-Jacques*

Contribution from the Département de Chimie, Université de Montréal, C.P. 6128, Succ. "A", Montréal, Québec, Canada H3C 3J7. *Received July 23, 1986*

Abstract: The object of this investigation is the experimental identification of the main contributing factors to the gauche conformational effect. The unique geometrical features and the flexibility of the seven-membered ring are used advantageously. The conformational changes caused by variation of the single halogen substituent at the 3-position of 1,5-benzodioxepin (**1**) are determined by quantitative dynamic NMR methods. The results show that the number of conformations varies from one to three (C_e, C_a, and TB) depending on the substituent electronegativity and solvent polarity. The trends observed for the four halogens and the methoxy group indicate that intramolecular stereoelectronic orbital interactions of the σ-σ^* type are most important for the heavier halogens (I, Br, and Cl). The increasing amount of the TB form from I to Cl is a direct consequence of the increase in overlap in the σ_{C-H}-σ^*_{C-X} interaction while the decreasing amount of C_e reflects on stabilization due to the σ_{C-X}-σ^*_{C-O} interaction. The F substituent shows a strong departure from the trends noted for the three other halogens, while the data for the methoxy group suggest a behavior intermediate between Cl and F. For these two more electronegative substituents, the situation appears more complex as several contributing factors come into play.

Recently reported NMR studies[1,2] on the conformations of 1,5-benzodioxepins have shown that both **1** and **2** exist as mixtures of chair (C) and twist-boat (TB) conformations whereby **1** favors

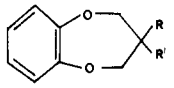

1; R = R' = H
2; R = R' = CH_3
3; R = H; R' = CH_3

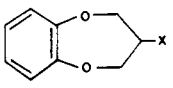

4; X = OCH_3
5; X = F
6; X = Cl
7; X = Br
8; X = I

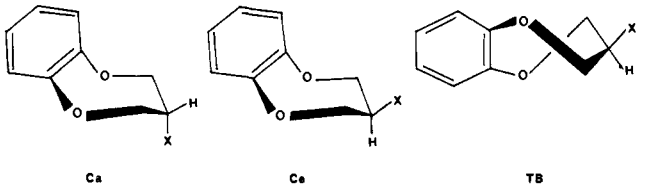

C_a C_e TB

the C form while **2** prefers the TB form. A marked difference was observed for the two monosubstituted derivatives investigated: the methyl derivative **3** exists as a mixture of three conformations, namely the chair with an equatorial methyl group (C_e), the axial chair (C_a), and the TB form, while the 3-methoxy derivative **4** reveals the presence of only two forms, C_a and TB, The latter is predominant in the polar solvent CHF_2Cl and becomes the sole conformation observed in the less polar solvent CH_3OCH_3.

These partial results have led to the present study of 3-halogenated derivatives of **1** in order to fully assess the conformational effect of single polar substituents and define the mechanism of the gauche conformational effect expected to exist in some of the conformations of these compounds. Previous reports[3-7] on this phenomenon have suggested that the underlying interactions can be either repulsive, negligible, or attractive depending on the nature of the two heteroatoms in a gauche disposition. Furthermore, recent theoretical studies[8,9] indicate that bond-antibond (σ-σ^*) orbital interactions in the O-C-C-X fragment are important so that the series of compounds **5-8** is expected to provide a unique molecular framework, resulting from

(1) Ménard, D.; St-Jacques, M. *J. Am. Chem. Soc.* **1984**, *106*, 2055.
(2) Ménard, D.; St-Jacques, M. *Can. J. Chem.* **1981**, *59*, 1160.
(3) Wolfe, S. *Acc. Chem. Res.* **1972**, *5*, 102.
(4) (a) Abraham, R. J.; Banks, H. D.; Eliel, E. L.; Hofer, O.; Kaloustian, M. K. *J. Am. Chem. Soc.* **1972**, *94*, 1913. (b) Kotite, N. J.; Harris, M.; Kaloustian, M. K. *J. Chem. Soc., Chem. Commun.* **1977**, 911.
(5) Zefirov, N. S.; Gurvich, L. G. *Tetrahedron* **1976**, *32*, 1211.
(6) Juaristi, E. *J. Chem. Educ.* **1979**, *56*, 438.
(7) Kirby, A. J. In *The Anomeric Effect and Related Stereoelectronic Effect at Oxygen*; Springer-Verlag: Berlin, Heidelberg, New York, 1983.
(8) Brunck, T. K.; Weinhold, F. *J. Am. Chem. Soc.* **1979**, *101*, 1700.
(9) Epiotis, N. D.; Cherry, W. R.; Shaik, S.; Yates, R. L.; Bernardi, F. *Top. Curr. Chem.* **1977**, 70.

0002-7863/87/1509-2616$01.50/0

Table I. Carbon-13 Chemical Shifts for Compounds **5–8** at High and Low Temperatures[a]

compd	solvent	temp (°C)	conformtn[b]	C-6,7	C-8,11	C-9,10	C-2,4[g]	C-3[g]
5 (X = F)	CHF_2Cl	−20		151.66	124.98	122.40	72.60 (J = 25.7)[c]	90.86 (J = 175.6)
		−125	Ca	153.28	126.54	123.76	72.89 (J = 19.6)	91.39 (J = 175.8)
			TB	150.13	124.42	121.87	72.01 (J = 27.3)	90.50 (J = 173.3)
	CH_3OCH_3	−20		151.14	124.11	121.83	72.19 (J = 26.7)	90.31 (J = 175.6)
		−132	Ca	153.49	125.58	123.35	72.36 (J = 19.5)	91.04 (J = 176.4)
			TB	150.18	123.77	121.44	71.61 (J = 27.3)	90.07 (J = 173.3)
6 (X = Cl)	CHF_2Cl	−25		151.71	125.15	122.47	75.47	56.93
		−120	Ce	152.77[d]	126.33	123.93	75.60	53.54
			Ca	152.99[d]	126.43	123.68	75.18	61.67
			TB	150.16	124.45	121.76	74.83	57.35
	CH_3OCH_3	−25		151.39	124.41	121.98	74.97	56.79
		−120	Ce	152.82	125.70	123.21	74.72	53.82
			Ca	152.82	125.70	123.21	74.72	*e*
			TB	150.14	123.79	121.31	74.36	57.55
7 (X = Br)	CHF_2Cl	−25		152.02	125.38	122.68	75.85	47.54
		−125	Ce	152.80	126.45	123.68	75.18	44.96
			Ca	152.89	126.31	124.05	75.18	*f*
			TB	150.13	124.50	121.79	75.55	48.66
	CH_3OCH_3	−25		151.72	124.64	122.19	75.33	47.78
		−120	Ce	152.86	125.63	123.14	74.69	45.63
			Ca	152.86	125.63	123.14	74.68	*f*
			TB	150.10	123.78	121.28	74.68	49.27
8 (X = I)	CHF_2Cl	−20		152.57	125.61	122.90	77.55	26.46
		−125	Ce	152.82	126.34	123.57	76.84	25.75
			Ca	152.67	126.13	124.14	76.84	35.57
			TB	150.04	124.43	121.72	76.84	27.05
	CH_3OCH_3	−20		152.43	124.93	122.51	77.10	26.81
		−130	Ce	153.10	125.51	123.09	76.18	25.87
			TB	150.18	123.75	121.28	76.46	26.96

[a] Solutions containing internal Me_4Si and CD_2Cl_2 (15–20%) for field lock purpose. [b] The symbols Ce, Ca, and TB refer to conformations described in the text. [c] Given in brackets are the C–F coupling constants. [d] The assignment of these two signals could be interchanged. [e] Signal overlaps with the CH_3OCH_3 solvent signal. [f] Signal overlaps with the CD_2Cl_2 signal. [g] J is measured in hertz.

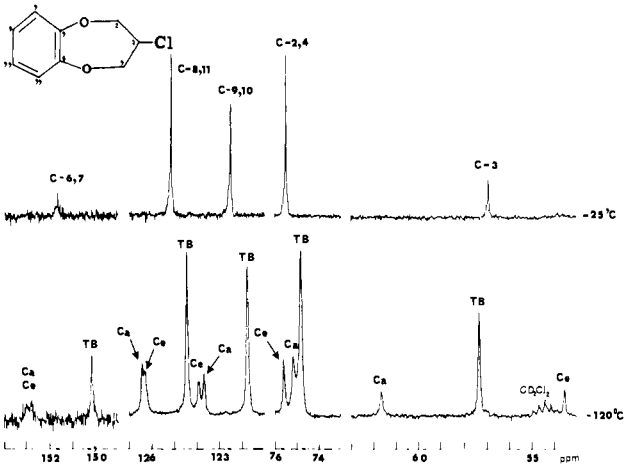

Figure 1. 100.62-MHz ^{13}C NMR spectra of **6** in CHF_2Cl at −25 and −120 °C (C_e = equatorial chair, C_a = axial chair, and TB = twist boat).

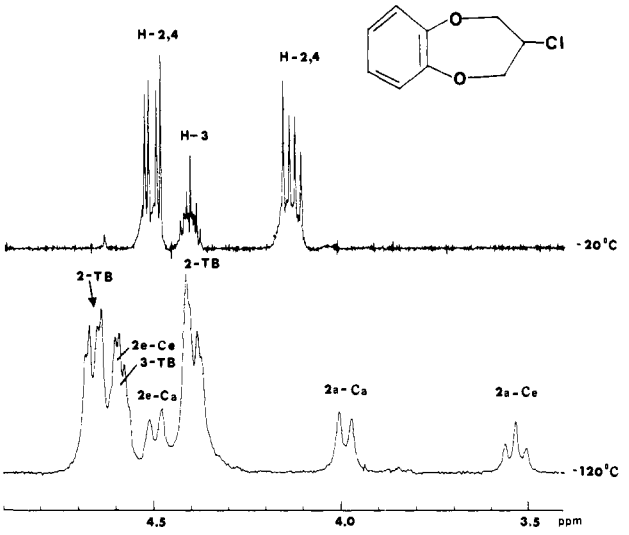

Figure 2. 400.13-MHz ^1H NMR spectra of the aliphatic protons of **6** in CHF_2Cl at −20 and −120 °C. The abreviations refer to protons environments described in the text.

the accrued stability of the TB form, to comprehend the conformational consequences of changing the substituent electronegativity.

Results and Spectral Analysis

All four compounds, **5–8** gave dynamic ^1H and ^{13}C NMR spectral changes at low temperatures. Because of additional coupling with the fluorine atom, the results for compound **5** will be presented last.

Figure 1 illustrates the 100.62-MHz ^{13}C spectral modifications observed for **6** (X = Cl) in CHF_2Cl. At low temperature (−120 °C) all carbon signals have split into three lines of unequal intensity. The assignment of the C-8 to C-11 and C-2,4 signals was made by integration and arguments to be presented next. The assigned chemical shifts are reported in Table I.

Earlier studies[1,2] on compounds **1–4** have shown that the C-6,7 signals constitute a probe for the identification of the ring conformation (C or TB) adopted. Because these carbons are quite remote from the site of substitution, their chemical shifts are not influenced significantly by the axial or equatorial orientation of the substituent in the chair form. For instance, at −142 °C, the C-6,7 signal of compound **1** at lower field (153.35 ppm) is characteristic to the chair form, while the highly field signal (151.01 ppm) corresponds to the TB form.

A comparison of the above reference chemical shifts with those determined for compound **6** at −120 °C (Table I and Figure 1) leads to the following assignment: the two close signals at 152.77 and 152.99 ppm represent the two C_a and C_e forms, while the signal at 150.16 ppm corresponds to the TB form which is the most abundant (63%).

In contrast, the C-3 region contains three well-resolved lines at 53.54, 57.35, and 61.67 ppm with an intensity ratio of 16:63:21, respectively. The signals at 53.54 and 61.67 ppm represent the C_a and C_e forms which are identified by the spectral analysis of the ^1H NMR spectra of compound **6** described below.

Table II. ^{1}H NMR Spectral Parameters for Compounds **5**–**7** at High and Low Temperatures

compd	solvent	temp (°C)	conformtn	H-2,4[e]	H-3[e]	H-8,11[a]
5 (X = F)	CHF_2Cl	−15		4.26 qd (J = −13.3, 25.1, 3.5) 4.45 td (J = −14.0, ~14.0, 4.4)	4.96 m ($^2J_{HF}$ = 47.2)	
		−120	Ca	3.85 dd (H-2, 4a) (J = −13.4, 40.7) 4.65 t (H-2, 4e) (J = 11–12)	4.84 m ($^2J_{HF}$ = 42.0)	
			TB	~4.50 (br) ~4.50 (br)	5.20 ($^2J_{HF}$ = 49.12)	
5	CF_2Cl_2	−20		~4.35 complex pattern	5.00 m ($^2J_{HF}$ = 48.4)	6.84 m
		−125	Ca	3.82 dd (H-2, 4a) (J = −13.9, 39.0)	4.84 m (J = 43.05)	7.05 s
			TB	*b*	5.16 m ($^2J_{HF}$ = 49.02)	6.84 s
6 (X = Cl)	CHF_2Cl	−20		4.13 dd (J = −12.6, 6.6) 4.51 dd (J = −12.6, 4.3)	4.40 m	
		−120	Ce	3.54 t ($J \approx$ 11–12) ~4.59[c]	*b*	
			Ca	3.99 d (H-2, 4a) (J = −13.5) 4.50 d (H-2, 4e) (J = −12.5)	*b*	
			TB	4.40 dd (J = −12.5, 4.3 Hz) 4.66 dd (J = −12.4, 4.7 Hz)	4.59 m	
6	CF_2Cl_2	−20		4.07 dd (J = −12.1, 6.6) 4.51 dd (J = −12.0, 4.2)	4.46 m	6.89 m
		−120	Ce	3.47 t (H-2, 4a) ($J \approx$ 10.1) 4.49 d (H-2, 4e) (J = −10.5)	~4.3[d]	7.04 s
			Ca	~4.40[d] ~4.35[d]	~4.35[d]	7.04 s
			TB	4.29 q (J = −12.8, 5.0) 4.57 q (J = −12.8, 4.8)	4.69 m	6.85 s
7 (X = Br)	CHF_2Cl	−10		4.08 dd (J = −12.5, 7.7) 4.56 dd (J = −12.6, 4.3)	4.42 m	
		−125	Ce	~3.59 t (H-2, 4a) (J = 11.7) ~4.63[c]	*b*	
			Ca	3.98 d (H-2, 4a) (J = −13.8) ~4.63[c]	*b*	
			TB	4.51 dd (J = −12.7, ~5.0) 4.71 dd (J = −12.9, ~5)	4.37 m	
7	CF_2Cl_2	−20		4.01 dd (J = −12.3, 7.9) 4.56 dd (J = −12.3, 4.4)	4.44 m	6.91 m
		−125	Ce	3.51 t (H-2, 4a) (J = 10–11) 4.53 d (H-2, 4e) (J = −10.5)	4.4	7.02 s
			Ca	~4.00 (br) *b*	*b*	7.02 s
			TB	~4.63 (br) ~4.72 (br)	4.33 m	6.84 s

[a] The aromatic protons overlap with the signals of the CHF_2Cl solvent and are reported only for the CF_2Cl_2 solvent. [b] The signals corresponding to the protons in the indicated conformation were not resolved. [c] This chemical shift was determined by selective homonuclear decoupling. [d] This chemical shift was determined from the analysis of the 2D-COSY spectrum. [e] J is measured in hertz.

The ^{1}H spectrum of **6** in CHF_2Cl at −20 °C (Figure 2) shows that the H-2,4 signals consist of two quartets centered at 4.13 and 4.51 ppm, while the H-3 signal is a multiplet at 4.40 ppm. These three signals change to give a complex spectrum at −120 °C. It has been possible to assign the majority of the signals by homonuclear decoupling and integration. The results are reported in Table II, and the main signals are identified in Figure 2. (Symbols 2_a-C_e refers to the axial proton at the 2- and 4-positions of the symmetrical C_e conformation, etc.). It is seen that the 2_a-C_e signal appears as a triplet (3.54 ppm) while the 2_a-C_a signal appears as a doublet (3.99 ppm) with an intensity ratio of 15:22, respectively. Selective irradiation at −120 °C of the 2_a-C_a doublet transforms the doublet at 4.50 ppm into a singlet, thus confirming that this signal arises from the 2_e-C_a protons of the C_a form. The splitting of these two doublets is due to the $^2J_{HH}$ coupling of −12.5 Hz. A second selective decoupling of the 2_a-C_e triplet (3.54 ppm) produces a change in the multiplicity of part of the signal at 4.59 and suggests that it is the chemical shift of the 2_e-C_e proton. Studies on 5-chloro-1,3-dioxane[10] have shown that the 2_e-C_a signal appears upfield from the 2_e-C_e signal (2_e-C_a = 4,02 and 2_e-C_e = 4.14 ppm), and the difference between these two chemical shifts is 0,12 ppm. The fact that chemical shift difference determined above between the two analogous protons in the spectrum of **6** at −120 °C is 0.09 ppm supports the assignment.

The signals of protons belonging to the TB form are more intense considering the predominance of this form for compound **6**, and the selective decoupling experiments produced no change for these signals. Considering that the pseudorotation process between the two equivalent forms of TB is still rapid on the NMR time scale[1] at −120 °C, then the characteristic signals of this conformation are averaged.[1] The signals of H-2,4 protons appear as two quartets at 4.66 and 4.40 ppm (signals identified by 2-TB in Figure 2), and the H-3 multiplet (3-TB) overlaps with the 2_e-C_e signal at 4,59 ppm. The H-3 signals of the C_a and C_e forms are not identified and are probably under the more intense signals of the TB form. The aromatic proton signals were not studied in CHF_2Cl because of interference from the solvent triplet in the same region.

This information can now be used to complete the ^{13}C NMR spectral analysis of compound **6** in CHF_2Cl at −120 °C (Figure 1). The integration indicates that for the C-3 region, the signal of the C_a form is at 61.67 ppm and that of the C_e form is at 53.54 ppm. Furthermore, the two C-2,4 chair signals were associated to the 2_a-C_e and 2_a-C_a protons by selective proton irradiation at −120 °C. The coupled ^{13}C signals appear as triplets which are perturbed as follows: When the proton triplet at 3.54 ppm is irradiated, the lower field C-2,4 triplet of the ^{13}C spectrum is collapsed, while irradiation of the proton doublet at 3.99 ppm collapses the higher field C-2,4 triplet. Thus, the C-2,4 signal of the C_e form is at lower field than that of the C_a form as shown in Figure 1. Integration leads to the ratio of 63:21:16 for the TB, C_a, and C_e forms, respectively, as summarized in Table III.

The ^{13}C spectral analysis of compound **6** in the less polar CH_3OCH_3 solvent, at low temperature, was made by comparison with the above results. At −120 °C, the C-3 signal of the C_a form

(10) Cazaux, L.; Chassaing, G.; Gorrichon, J.-P.; Maroni, P.; Prejzner, I. *Bull. Soc. Chim.* **1976**, 563.

Table III. Percentage[a] of the Conformations of Compounds 3–8 Detected at Low Temperature (−120 to −130 °C)

compd	solvent	Ca	TB	Ce
3	CHF_2Cl	10[b]	58	32
(CH_3)	CH_3OCH_3	9	49	42
4	CHF_2Cl	33[b]	67	
(OCH_3)	CH_3OCH_3		100	
5	CHF_2Cl	66	34	
(F)	CH_3OCH_3	30	70	
6	CHF_2Cl	21	63	16
(Cl)	CH_3OCH_3	4	77	19
7	CHF_2Cl	17	51	32
(Br)	CH_3OCH_3	6	54	40
8	CHF_2Cl	9	22	69
(I)	CH_3OCH_3		17	83

[a] The uncertainty in the conformation populations given is estimated to be ±2%. [b] Data for 3 and 4 taken from ref 1.

overlaps with the intense solvent signal so that the population ratio cannot be determined directly by one integration. The amount of each conformation was obtained indirectly as follows: The integration of the aromatic region gives a ratio for the TB (77%) and the combined C (23%) forms, while the integration of the C-3 region yield 19% for C_e relative to TB fixed at 77%. The C_a amount (4%) is then the difference between the C and C_e signals, and the population ratio of the three conformers is calculated to be 77:4:19 for TB, C_a, and C_e, respectively.

The ^1H spectral analysis of compound 6 at low temperature in the relatively nonpolar CF_2Cl_2 solvent indicates that it exists in a 75:6:19 ratio for the TB, C_a, and C_e form, respectively. CF_2Cl_2 was used instead of CH_3OCH_3, because the signals of the latter fall in the same region as those of 6. Furthermore, because of a small chemical shift solvent effect on changing from CHF_2Cl to CF_2Cl_2, it is possible to see clearly the multiplicity of the H-3 signal in the latter solvent. In this solvent, two aromatic signals are observed: one at 7.04 ppm (25%) representing the two chair forms and another at 6.85 ppm (75%) representing the TB form. The proportion of each of the two chair forms is obtained by integration of the 2_a-C_a and 2_a-C_e signals and then normalization to give 6% for the C_a form and 19% for the C_e form. Therefore, in the CF_2Cl_2, the populations are similar to those determined by ^{13}C NMR in CH_3OCH_3.

An alternative to the decoupling experiments is provided by the 2D COSY experiment[11] which enabled the assignment of all signals in the ^1H spectrum of 6 in CF_2Cl_2 at −120 °C. The results are reported in Table II, and Figure 3 shows the 2D COSY contour spectrum of 6 at −120 °C in CF_2Cl_2. The off-diagonal signals represent correlations between coupled protons whose chemical shifts are obtained from the diagonal line. Thus, the triplet at 3.47 ppm (2_a-C_e) shows two correlation signals 1 and 2 at 4.30 and at 4.49 ppm. Knowing that proton 2_a-C_e and H-3 couple with the 2_e-C_e proton, it is reasonable to say that the doublet at 4.49 ppm arises from the 2_e-C_e protons ($^2J_{HH}$ = −10.5 Hz), whereas the correlation at 4.30 ppm identifies the position of the 3-C_e signal which overlaps with other signals. The identification of the doublet at 4.49 ppm was confirmed by selective proton decoupling whereby irradiation of the triplet at 3.47 ppm transformed the doublet into a singlet. Decoupling experiments gave no additional useful information, whereas the 2D COSY spectra led to the assignment of the protons for these less abundant C_a form.

The signal at ~4.0 ppm represents the 2_a-C_a protons. Only one correlation (numbered 3 in Figure 3) is found at ~4.35 ppm; this observation suggests that the signals of 2_e-C_a and 3-C_a protons, both coupled to the 2_a-C_a protons, are situated at the same position. It is interesting to recall that in CHF_2Cl (Figure 2), the 2_e-C_a signal was resolved contrary to Figure 3 where it has shifted upfield to overlap with several other signals, On the other hand, the 2_e-C_e signal not resolved in CHF_2Cl is clearly seen in CF_2Cl_2 (Figure 3).

(11) Bax, A.; Freeman, R. *J. Magn. Reson.* **1981**, *44*, 542.

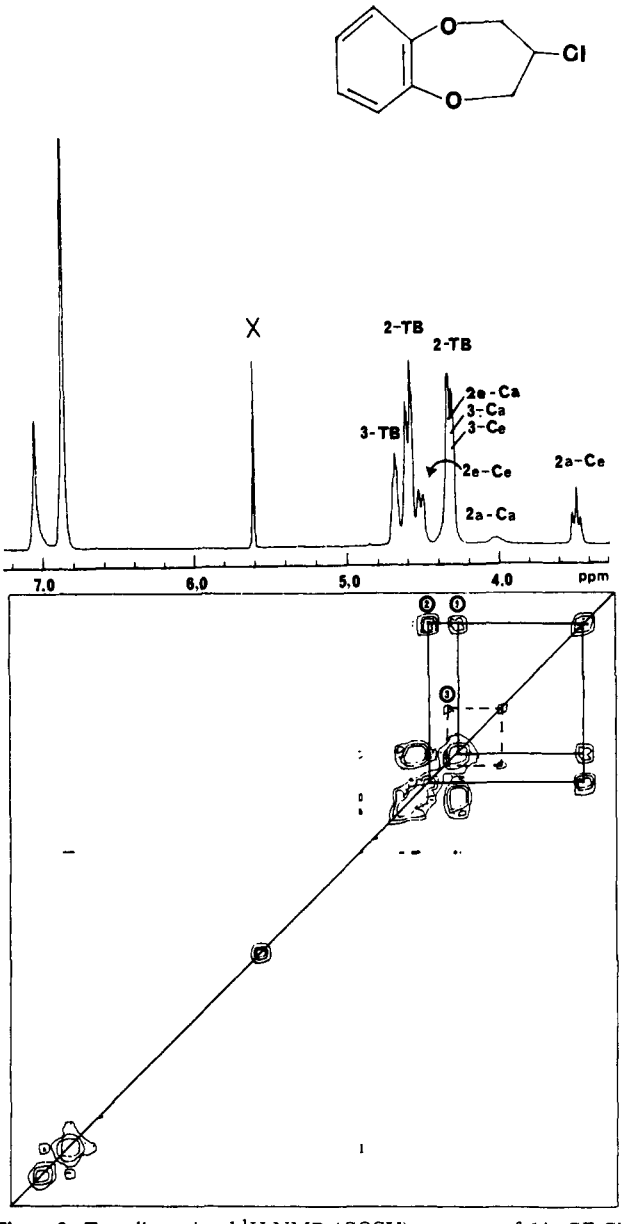

Figure 3. Two-dimensional ^1H NMR (COSY) spectrum of 6 in CF_2Cl_2 at −120 °C (× denotes impurity).

The ^1H signals of the TB form have been identified with the procedure used for Figure 2. The signals of the H-2,4 protons (abbreviated 2-TB in Figure 3) are two quartets at 4.29 and 4.57 ppm, and a multiplet at 4.69 ppm represents the H-3 proton of this same form (3-TB).

Similar spectral modifications have been observed in the ^1H and ^{13}C spectra of 7 (X = Br) and 8 (X = I) as well as 5 (X = F). Figures depicting spectral changes and analyses are available as Supplementary Material. The results are summarized in Tables I, II, and III.

Discussion

As summarized in Table III, the number of conformations observed for the series of compounds 4–8 varies from one to three depending on the nature of the polar substituent and on the solvent polarity. Previous results[1] suggest that such striking differences originate from a combination of molecular interactions involving both the substituents and the ring oxygen atoms. Expected to be prominent are the following factors: intramolecular electrostatic interactions, stereoelectronic orbital interactions between vicinal polar bonds, and solvation, These interactions have been described from a theoretical perspective and from experimental observations made mostly on 1,2-disubstituted ethanes and on six-membered heterocyclic molecules.

Published considerations suggest that polar substituents ought to be subdivided into two subgroups with regards to the gauche conformational effect. Indeed, it has been proposed[4,5] that an attractive interaction stabilizes a gauche arrangement for vicinal polar bonds in a –O–C–C–X moiety when X = OCH_3 and F, whereas the underlying interaction might be negligible or repulsive for the other three substituents; Cl, Br, and I. In addition, because **6**, **7**, and **8** most frequently show the presence of three conformations (TB, C_a, and C_e) and because signals for the C_e form have not been detected for **4** and **5**, the following analysis will consider **4** and **5** as a subgroup and **6–8** as another subgroup.

Because solvation effects are expected to be weaker in nonpolar solvents,[12] the results obtained for CH_3OCH_3 solutions are usually analyzed first. The observations made for **4** (X = OCH_3) were explained[1] as follows: **4**-TB (this symbol represents the TB form of **4**), the only conformation detected in dimethyl ether solution, is stabilized intramolecularly by both dipolar electrostatic interactions and bond–antibond (σ–σ^*) orbital interactions, whereas **4**-C_a is destabilized by dipolar interactions which oppose and essentially neutralize the stabilizing bond–antibond interactions. In addition, the change in solvent (from dimethyl ether to the more polar CHF_2Cl) shifts the **4**-TB $\rightleftharpoons$ **4**-C_a equilibrium to the right as the result of an attenuation of the electrostatic interactions and better solvation of the more polar **4**-C_a form. In contrast, the **4**-C_e form has not been observed in either of the solvents used, because it is not stabilized by any of these factors.

Table III shows that the major difference between the data for **4** and **5** (X = F) is roughly a 30% increase in the amount of the **5**-C_a form and a concomitant decrease of **5**-TB. This shift is in agreement with the well-documented phenomenon associating stabilization to the O/F gauche arrangement to a special attraction.[6] Stronger stabilization has also been observed experimentally for the C_a form of 2-isopropyl-5-fluoro-1,3-dioxane.[13] The nature of the interactions involved for F will be discussed after the behavior of **6–8** is analyzed.

In contrast to **4** and **5**, the compounds of the second subgroup (**6**, **7**, and **8**) are characterized by the presence of the C_e form in both solvents. The existence of three conformations makes the analysis somewhat more complex relative to the six-membered cyclic analogues,[4,5] and it becomes a more tedious task to sort out the various attractive or repulsive contributors for the O/Cl, O/Br, and O/I situations encountered in **6–8**. For example, compound **6** (X = Cl) exists as a mixture of three conformations among which the **6**-TB form predominates in both the more polar CHF_2Cl and the less polar CH_3OCH_3 solvents. By comparison, results for the analogous 2-isopropyl-5-chloro-1,3-dioxane[10] show the existence of only two conformations, C_a and C_e. In this six-membered cyclic compound, the C_e form is preferred over C_a, and a reduction in solvent polarity ($CHCl_3$ to diethyl ether) further increases the C_e amount. In contrast, for the seven-membered analogue, the solvent change (CHF_2Cl to dimethyl ether) shows little effect on **6**-C_e while producing a strong decrease in **6**-C_a to compensate for a rise in **6**-TB.

Conformational Populations and Substituent Electronegativity. An overall picture of the behavior of the seven-membered cyclic compounds **4–8** is provided by Figure 4 where conformation populations in Table III are plotted against the electronegativity[14] of each of the substituents. Lines are drawn between the data points for each conformation of the four halogenated compounds to illustrate the effects of substituent change on each conformation. Points for the OCH_3 substituent of **4** are joined to the others by a broken line, and the data for **4** will be considered separately from those of the four halogenated compounds **5–8**. Whereas the amount of C_a for the four halogens shows a gradual increase from I to F, the lines drawn for C_e and TB show linear behaviors for I, Br, and Cl with sharp breaks for F. Here F is seen to behave differently from the other three halogen substituents.

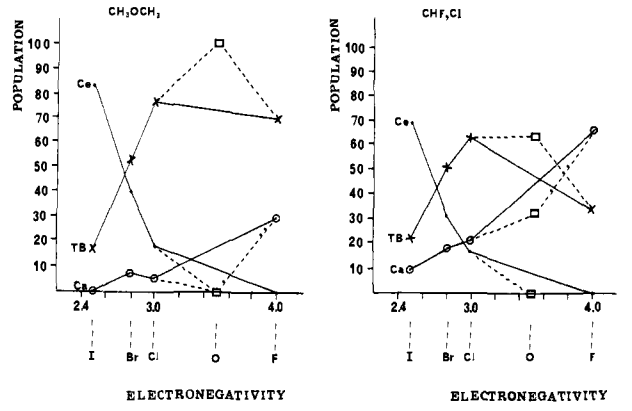

Figure 4. Plots of the population of the C_e form (●), C_a form (○), and TB form (×) vs. the electronegativity of I, Br, Cl, and F in CH_3OCH_3 and CHF_2Cl solutions. Data for OCH_3 are represented by a □ and joined to the others by broken lines.

From a phenomenological point of view, the analysis of Figure 4 for the four halogens is complex. Inversion of relative stabilities of the C_e and C_a forms is seen to occur between Cl and F in the CH_3OCH_3 solution whereas, for the C_e and TB forms, it occurs between I and Br. No crossover exists between the TB and C_a lines. Changing the solvent to the more polar CHF_2Cl leads to three crossover points: the C_e-TB one still occurs between I and Br while that between C_e and C_a now takes place between Br and Cl. In addition, the relative stabilities of the C_a and TB forms are inverted between Cl and F.

From studies of 1,2-disubstituted cyclohexane derivatives, Zefirov and co-workers[5] have claimed that the conformational behavior arising from the vicinal gauche pairs O/Cl, O/Br, and O/I can be adequately interpreted in terms of steric and polar interactions. Unfortunately, the approximations used to arrive at that conclusion do not justify direct extrapolation to compounds **6–8**, the members of our second subgroup. A critical analysis of anticipated differences in steric and electrostatic interactions for Cl, Br, and I is therefore required.

Steric differences for the three heavier halogens should be reflected by the equatorial preference noted for cyclohexyl halides.[15] Best values for the $-\Delta G^\circ$ parameter (A values) chosen by Zefirov[5] are 0.5 ± 0.1 (Cl), 0.48 ± 0.1 (Br), and 0.45 ± 0.1 (I). The great similarity between these values suggests the steric factor ought not to be the prime contributor to the trends noted for **6–8** in Figure 4.

Electrostatic interactions are more difficult to assess quantitatively because the calculations of contributions from dipoles and quadrupoles are subject to serious limitations[16] owing to the approximation used and to the absence of precise geometrical information for the three conformers of molecules **6–8**. Although such calculations were able to account for the effect of variation of solvent dielectric for 5-substituted derivatives of 2-isopropyl-1,3-dioxane,[4] we feel that in the present study a qualitative approach is less subject to criticism.[16,17] We will therefore concentrate on intramolecular dipolar interactions and solvation in light of the simple two terms formalism used to explain the conformational features of derivatives[12,18] of 1,3-dioxane with polar substituents at C-5. The first term, E_S, is the solvation energy (maximum in polar solvent and zero in gas phase), and the second term, E_D, is the sum of energies of intramolecular electrostatic interactions E_d between the molecular dipoles. E_D can be stabilizing or destabilizing depending upon the relative orientations of each bond dipole; it tends toward zero in polar solvent and becomes important in the gas phase.

(12) Kaloustian, M. K. *J. Chem. Educ.* **1974**, *51*, 777.
(13) Mager, S.; Eliel, E. L. *Rev. Roum. Chim.* **1973**, *12*, 2097.
(14) Pauling, L. In *The Chemical Bond*; Cornell University Press: Ithaca, New York, 1967.
(15) Jensen, F. R.; Bushweller, C. H.; Beck, B. H. *J. Am. Chem. Soc.* **1969**, *91*, 344.
(16) Lambert, J. B.; Taba, K. M. *J. Am. Chem. Soc.* **1981**, *103*, 5828.
(17) Ménard, D.; St-Jacques, M. *Tetrahedron* **1983**, *39*, 1041.
(18) Kaloustian, M. K.; Dennis, N.; Mager, S.; Evans, S. A.; Alcudia, F.; Eliel, E. L. *J. Am. Chem. Soc.* **1976**, *98*, 956.

The interaction energy E_d between two unpolarizable points dipoles μ_1 and μ_2 is given by[12]

$$E_d = 3(\mu_1 \mathbf{r})(\mu_2 \mathbf{r})/\mathbf{r}^5 + \mu_1\mu_2/\mathbf{r}^3 \qquad \text{and } E_D = \Sigma E_d$$

where $\mathbf{r}$ is the vector joining the midpoints of interacting dipoles μ_1 and μ_2.

This equation indicates that the important terms are μ, $\mathbf{r}$, and the angle between the interacting dipoles. The fact that the three carbon–halogen bond dipole moments are quite similar for I, Br, and Cl (2.2–2.3 D)[4,19] suggests that the μ parameter (bond dipole moment) is constant as are the angles between the dipole orientations in each conformation. Because the A values are almost the same for I, Br, and Cl, the electron cloud about each halogen atom should be similarly located in a given conformation relative to the ring oxygens so that the distance between the dipoles should be similar. Therefore, the E_D term cannot explain the trends observed in Figure 4.

Contrary to an earlier suggestion based on a study of six-membered cyclic compounds,[5] steric and dipolar interactions cannot explain the data obtained for **6–8**. In addition, the fact that Figure 4 shows similar trends for the three conformations in both CH_3OCH_3 and CHF_2Cl indicates that solvation is not fundamentally responsible for the slopes characterizing each conformation. The more recent concepts of stereoelectronic theory[7] suggest that bond–antibond (σ–σ^*) orbital interactions[9,20] could be effective in some of the conformations of compounds **6–8**.

Stereoelectronic Bond–Antibond Orbital Interactions. Interaction between orbitals can be stabilizing or destabilizing depending upon orbital occupancy. In general, the interaction between an occupied and an unoccupied orbital is stabilizing.[20,21] The presently acceptable level of perturbation molecular orbital theory[7,8] predicts that in molecules with fragments such as X–C–C–Y a bond–antibond interaction is most effective for a trans arrangement of the C–X and C–Y bonds and that stabilization increases when the antibonding orbital σ^* energy decreases and when the bonding orbital σ energy increases. As a result, the stereoelectronic interaction force is generally determined by two contributions: the energy difference (ΔE) between the σ and σ^* orbitals involved and the orbital overlap. As a first approximation, the smallest energy difference has been used to identify the dominant interaction (the most stabilizing) for simple cases.[9,21] While this effect is small in an absolute sense, it is of the order of magnitude of torsional energy barriers which determine the relative stability of the possible ring conformations.[8]

The relevant orbitals and their relative energy levels are shown schematically in Figure 5. The order of the σ^* orbitals is the result of CNDO/2 calculations[9] and the following generalization: (a) Down a column of the periodic table the energy decreases (I < Br < Cl < F) and (b) along a row, the energy also decreases to the right and thus σ^*_{C-O} lies higher in energy than the σ^*_{C-F} orbital. The ordering of the σ orbitals in suggested by ab initio and CNDO/2 calculations[9] and is supported by the analysis of ionization potentials of CH_3X molecules.[22,23] Obviously, this approach does not provide an energy scale connecting all the orbitals given. As a consequence, it is not possible to determine accurate energy differences between the possible pairs of σ–σ^* orbitals, and only a qualitative discussion is possible without elaborate molecular orbital calculations.[8,9]

The stability resulting from a σ–σ^* interaction is proportional to $S^2/\Delta E$ where S is the orbital overlap and ΔE is the energy difference between the σ and the σ^* orbitals.[21] Furthermore, overlap is sensitive[24] to changes in the electronegativity of X

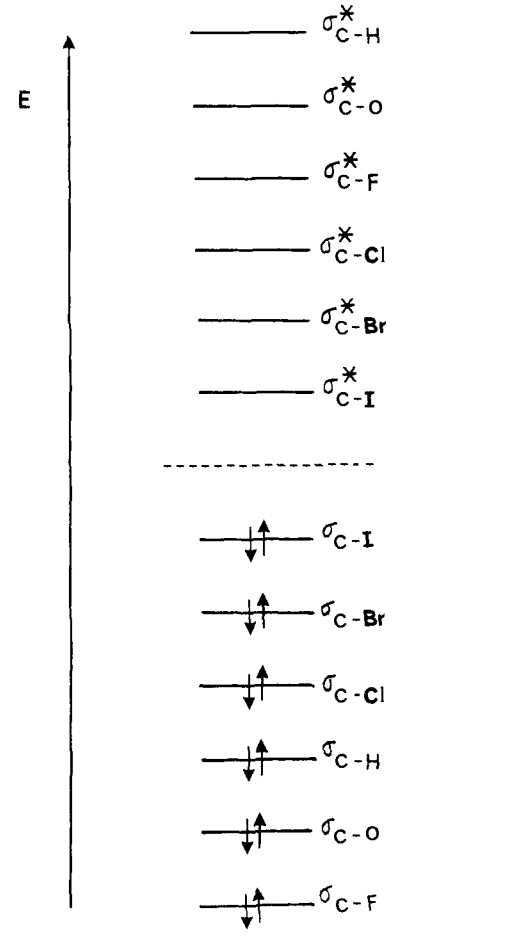

Figure 5. Order of bond and antibond orbital energies of C–X bond in various $X–CH_2CH_2–Y$ and CH_3X molecules.

through either the σ^*_{C-X} or the σ_{C-X} orbitals, but the effect is opposite for each orbital. For example, an increase in electronegativity of X increases the electronic density of the σ^*_{C-X} orbital near C so that better overlap results,[8,24] while for σ_{C-X} charge density is displaced[25] away from C toward X and overlap is weakened.

Our objective is now to analyze the effect of substituent change for each of the three possible conformation, first for X = I, Br, and Cl in light of the above theoretical framework. This approach keeps most geometric parameters constant and enhances the probability of identifying the interactions inherent to the substituents.

Projections about the C(3)–C(2) bond (or the C(3)–C(4) bond) for the symmetrical C_e and C_a forms are shown by structures **9** and **10**, respectively, together with the σ–σ^* interactions involving the polar bonds. Projection **9** for C_e shows that the C–O and C–X bonds are antiperiplanar; the dominant interaction is therefore σ_{C-X}–σ^*_{C-O} (because of symmetry, two such interactions exist). Figure 5 indicates that the energy of the σ_{C-X} orbital decreases from I to Cl and that, as a consequence, ΔE for the σ_{C-X}–σ^*_{C-O} interaction increases from I to Cl. Because overlap[25] from the σ_{C-X} orbital is expected to decrease from I to Cl, both terms (ΔE and S) contribute to the reduced stability of the C_e forms, in agreement with the essentially linear decrease in the C_e amount noted in Figure 4. Estimates of the relative contribution from each term will require elaborate and accurate calculations.

This context suggests that two sources might contribute to the departure from linearity observed for F in the C_e line of Figure

(19) McClellan, A. L. *Tables of Experimental Dipole Moments*; W. H. Freeman: San Francisco, 1963; p 210.
(20) Epiotis, N. D.; Yates, L. R.; Larson, J. R.; Kirmaier, C. R.; Bernardi, F. *J. Am. Chem. Soc.* **1977**, *99*, 8379.
(21) Albright, T. A.; Burdett, J. K.; Whangho, M. *Orbital Interactions in Chemistry*; John Wiley & Sons: New York, 1985.
(22) Bingham, R. C. *J. Am. Chem. Soc.* **1975**, *97*, 6473.
(23) Kimura, K.; Ktsumata, S.; Achiba, Y.; Amazaki, T. Y.; Iwaka, S. *Handbook of Hel Photoelectron Spectra of Fundamental Organic Molecules*; Japan Scientific Societies Press: Tokyo, Halsted Press: New York, 1981.
(24) Minkine, V.; Simkine, B.; Mihiaev, R. *Théorie de la Structure Molēculaire (Couches Ēlectroniques)*; French translation Mir.: Moscow, 1982; pp 132, 249, 250.
(25) (a) Weinhold, F.; Brunk, T. K. *J. Am. Chem. Soc.* **1976**, *98*, 3745. (b) Reed, A. E.; Weinstock, R. B.; Weinhold, F. *J. Chem. Phys.* **1985**, *83*, 735.

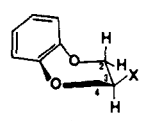

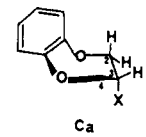

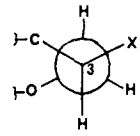

9

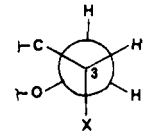

10

a) X = Cl, Br, I → $2(\sigma_{C-X} - \sigma^*_{C-O})$ $2(\sigma_{C-H} - \sigma^*_{C-X})$ $2(\sigma_{C-H} - \sigma^*_{C-O})$

b) X = F → $2(\sigma_{C-O} - \sigma^*_{C-F})$ $2(\sigma_{C-H} - \sigma^*_{C-F})$ $2(\sigma_{C-H} - \sigma^*_{C-O})$

4. First, the steric and electrostatic interactions are not similar to those of the other three halogens, and, second, the dominant orbital interaction in **5**-C_e is predicted to be different, namely the weaker σ_{C-O}–σ^*_{C-F} interaction.

It is also important to note that because the C_e population is essentially zero for F, the straight line joining Cl and F has no physical meaning. In fact, no C_e form was detected[1] for **4** (X = OCH_3) even though the electronegativity of oxygen falls between Cl and F as is also shown in Figure 4, Although the trend noted for OCH_3 is in line with predictions from consideration of the orbital interactions, the departure from linearity for the substituents of the first subgroup (X = OCH_3 and F) indicates that the situation is more complex relative to the second subgroup (X = Cl, Br, I) for which the essentially linear behavior can be attributed to orbital interactions as the main source of differentiation.

With regards to C_a, projection **10** reveals that there are two bond–antibond interactions involving the polar bonds, Since σ_{C-H}–σ^*_{C-O} is independent of X, it cannot explain the trend observed. Hence, the dominant interaction must be σ_{C-H}–σ^*_{C-X}. Indeed, this interaction is expected to be significant because σ_{C-H} is a relatively good donor[8] as is seen from its position in Figure 5. The increase in ΔE predicted for this interaction as X changes from I to Cl is opposed by the increased overlap accompanying the increasing electronegativity. The upward trend for C_a in Figure 4 indicates that the overlap contribution is overriding and that σ_{C-H}–σ^*_{C-X} is overall more stabilizing for Br and Cl than for I. The fact that Figure 4 shows a slightly smaller amount of C_a for Cl than for Br in CH_3OCH_3 may arise from a greater competition between the two opposing ΔE and S^2 terms. However, the small populations present and the small difference involved do not justify a quantitative interpretation.

Table III shows that there is no **4**-C_a (X = OCH_3) present in CH_3OCH_3. Part of the deviation noted for the OCH_3 points in Figure 4 could result from a change in dipole orientation. Whereas the dipole moment of the halogen substituents is located along the C–X bond, that of the methoxy group bisects the C–O–C angle of the most stable rotamer. In addition, electrostatic interactions destabilize **4**-C_a and could overcome the stabilization expected from the weak σ_{C-O}–σ^*_{C-O} orbital interaction.

The solvent change from CH_3OCH_3 to the more polar CHF_2Cl solvent increases all C_a populations and straightens the C_a line so that a gradual upward trend is now observed in Figure 4, Although the general upward trend is in line with the dominance of overlap in σ_{C-H}–σ^*_{C-X} for all five substituents, other contributions are important for F and OCH_3. The solvent change is expected to attenuate the intramolecular dipolar interactions[12] and stabilize the more polar C_a form through better solvation. As a result, the deviation for OCH_3 is less pronounced, and electrostatic differences relative to the halogens could contribute to the small dip observed. Previous results[1] for compound **2** (CH_3) summarized in Table III show an appreciable amount (~10%) of the C_a form in both solvents. The fact that steric repulsion is weak for the methyl group in **2** suggests that it is probably not a very important contributor to the differences noted for **4**–**8**.

In contrast, the solvent change to a more polar one has not modified the overall shape of the C_e line in Figure 4 although all populations have decreased (Table III). This is compatible with the dominance of orbital interactions for X = I, Br, Cl whereas for F and OCH_3, the absence of the C_e forms suggests that stabilization from orbital interaction is relatively unimportant.

Turning to the behavior noted for TB in Figure 4, we see a linear increase from I to Cl and a sharp break for F. This observation is essentially the opposite of that for C_e discussed earlier. Here also we will consider the heavier halogens first. Structures **11** and **12** illustrate projections about the C(3)–C(2) and C(3)–C(4)

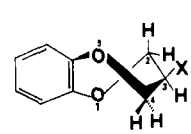

TB

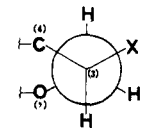

11

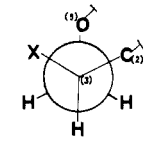

12

I, Br, Cl → σ_{C-X} - σ^*_{C-O} σ_{C-H} - σ^*_{C-X} σ_{C-H} - σ^*_{C-O}

F → σ_{C-O} - σ^*_{C-F} σ_{C-H} - σ^*_{C-F} σ_{C-H} - σ^*_{C-O}

bonds, respectively, of TB. The fact that the trend noted for TB in Figure 4 is opposite to that characterizing C_e suggests that the σ_{C-X}–σ^*_{C-O} interaction in **11** is less important than σ_{C-H}–σ^*_{C-X} existing in **12**. Indeed, the latter interaction is expected to be effective from Figure 5, and the overlap increase with electronegativity could account for the essentially linear upward trend from I to Cl. The fact that both the C_a and TB lines show upward trends for I to Cl is supportive since the same interaction is dominant for both conformations. The difference in slope should not be too surprising, because it probably reflects the fact that the C_a form is appreciably puckered so that the C–H and the C–X bonds are not perfectly antiperiplanar. In contrast, the TB form is highly flexible so that optimum geometry for maximum orbital interaction can be attained.

The departure for F in the TB line of Figure 4 suggests that factors other than the σ_{C-H}–σ^*_{C-F} interaction are operative, because this orbital interaction is expected to provide more stabilization for F relative to Cl from increased overlap unless the two terms, S^2 and ΔE, no longer compensate in the same way in the σ_{C-H}–σ^*_{C-X} interactions for substituents of the two subgroups. Differences in electrostatic interactions (E_D and E_S) for F may therefore be at the origin of the break in the TB line as was the case for the C_e line. The fact that the overall effect for F arises from a delicate balance of several contributions in three conformations makes a quantitative rationalization very difficult. Nevertheless, the observation that the TB amount for **4** (X = OCH_3) deviates in the same direction as F suggests that additional factors to orbital interactions are operative for these two more electronegative substituents.

While the overall shape of the TB line in Figure 4 is not changed on going from CH_3OCH_3 to CHF_2Cl, **5**-TB (X = F) is more destabilized relative to X = Cl and Br in CHF_2Cl than in the less polar solvent CH_3OCH_3. Better solvation of the more polar C_a

conformation in CHF_2Cl should favor **5**-C_a over **5**-TB, Furthermore, the attenuation of destabilizing E_D interactions in C_a and smaller E_S and E_D interactions in TB should also favor **5**-C_a, These two combined effects rationalize the crossover in C_a and TB lines observed in CHF_2Cl.

Concluding Remarks. In conclusion, we can state that intramolecular orbital interactions explain the general trends observed for the conformation populations of **6**, **7**, and **8** illustrated in Figure 4. The deviations noted for the more electronegative substituents F (**5**) and OCH_3 (**4**) result from a serious competition between σ–σ^* and dipolar interactions for the TB and C_a forms. The σ–σ^* interactions are weaker in the C_e form which is not detected for these two compounds. The fact that only two forms are observed for **4** and **5** allowed a clearer observation of the solvation effect accompanying the solvent change, The results for the series **4**–**8** therefore provide a good assessment of the forces at the origin of the so-called attractive and repulsive gauche conformational effects. The relative importance of the various contributors is not easy to determine, but our results demonstrate that a description of each one is necessary for extrapolations to more complex flexible systems. In this regard, the three conformations of the seven-membered ring provide a most convenient probe for the experimental testing of future more elaborate theories on the gauche effect.[26]

Experimental Section

Melting points are uncorrected and were detemined with a Thomas Hoover (uni-melt) melting point apparatus. High resolution spectra at 70 eV were recorded by using a modified MS-9 spectrometer.

Routine ^1H NMR spectra were taken on a Bruker WH-90 spectrometer: solutions were typically 10% (w/v) in $CDCl_3$ containing Me_4Si as reference.

The variable temperature ^1H NMR spectra at 400.13 MHz and ^{13}C NMR spectra at 100.62 MHz were obtained by using a Bruker WH-400 spectrometer equipped with a variable temperature unit B-VT-1000. Calibration using a thermocouple inside a solvent-containing NMR tube indicates that the low temperatures reported are exact within 3 °C.

All ^{13}C NMR spectra were recorded with broad-band proton decoupling, and the following instrumental parameters used are typical: flip angle: 79°; SW = 20 000 Hz; data size = 16 K; AQ = 0.41 s. The spectra were recorded as solutions in CHF_2Cl or CH_3OCH_3 (80–150 mg in 2.2 mL of solution) containing Me_4Si and about 15–20% of CD_2Cl_2 as locking agent, in standard 10-mm tubes which had been degassed and sealed. For proton, the typical instrumental parameters used are as follows: flip angle = 30°–87°; SW = 5000 Hz; data size = 8 and 16 K; AQ = 0.90–1.82 s.

Integrations were carried out by using the Bruker software. The uncertainty is estimated as ±2% from standard deviation calculations.[27]

^1H NMR spectra were recorded as solutions in CHF_2Cl or CF_2Cl_2 (5–10 mg in 0.55 mL of solution) containing Me_4Si and about 15–20% of CD_2Cl_2 or CD_3COCD_3 (for locking purpose), in standard 5-mm tubes which were degassed and sealed.

For the 2D COSY experiment, the following pulse sequence was used: RD-90°-t_1-45°-acq. A spectral width of 1901 Hz was used with quadrature detection to collect a 80 Fid × 1 K data matrix. The matrix was zero-filled in the t_1 dimension and transformed in the magnitude mode by using the sine-bell square function. Digital resolution in the resulting 256 × 1 K data matrix was 3.7 Hz per point.

2*H*-2,3-Dihydro-3-mesyl-1,5-benzodioxepin. To a solution of 1.4 g (0.0084 mol) of 2*H*-2,3-dihydro-3-hydroxy-1,5-benzodioxepin[1] in 100 mL of anhydrous dichloromethane was added dropwise 1.77 mL of triethylamine and 0.98 mL (0.013 mol) of methanesulfonyl chloride. The mixture was stirred at room temperature for 1 h. The solution was washed with 2 × 75 mL of cold water, 2 × 75 mL of cold HCl 10%, 2 × 75 mL of cold saturated solution $NaHCO_3$, and 2 × 75 mL of cold drine. The organic fractions were dried over $MgSO_4$, filtered, and evaporated. A yellow solid was obtained: 1.41 g (69%); ^1H NMR δ ($CDCl_3$), 3.13 (3 H, s, CH_3), 4.46 (4 H, d, CH_2), 5.26 (1 H, m, CH), 6.95 ppm (4 H, s, Ar).

2*H*-2,3-Dihydro-3-fluoro-1,5-benzodioxepin (5), A mixture of 4.0 g (0.016 mol) of 2*H*-2,3-dihydro-3-mesyl-1,5-benzodioxepin and 8.7 g (0.15 mol) of KF in 150 mL of diethylene glycol was heated at 150 °C for 16 h. When the solution was cooled at room temperature, 200 mL of brine was added. The solution was then extracted with ether, and the organic fraction was dried with $MgSO_4$, filtered, and evaporated. The product was purified by flash chromatography on silica gel by using 70% hexane and 30% dichloromethane as eluent giving 0.8645 g (32%) of a white solid: mp = 40 °C; ^1H NMR δ ($CDCl_3$) 4.35 (2 H, q, CH_2), 4.65 (2 H, d, CH_2), 5.03 (1 H, td, CH), 6.95 (4 H, s, Ar); mass spectrum calcd for $C_9H_9O_2F$, M 168.0566, found (70 eV) 168.0594 $(M)^+$, 149 $(M-F)^+$, 135 $(M-F-CH)^+$, 121 $(M-F-CH-CH_2)^+$.

2*H*-2,3-Dihydro-3-chloro-1,5-benzodioxepin (6), A solution of 1.0 g (0.006 mol) of 2*H*-2,3-dihydro-3-hydroxy-1,5-benzodioxepin in 100 mL of anhydrous dichloromethane and 1.64 g (0.012 mol) of *N*-chlorosuccinimide was cooled at 0 °C. Afterwards, 3.16 g (0.012 mol) of triphenylphosphine in 30 mL of dichloromethane was added dropwise, and the solution was refluxed for 16 h. The dichloromethane was evaporated, and the product was distilled under reduce pressure. A colorless liquid was obtained: 0.72 g (64%); ^1H NMR δ ($CDCl_3$) 4.62–4.03 (5 H, m, CH_2–O + CH), 6.95 (4 H, s, Ar); mass spectrum calcd for $C_9H_9O_2Cl$, M 184.02911, found (70 eV) 184.0289 $(M)^+$, 149 $(M-Cl)^+$, 121 $(M-Cl-CH-CH_2)^+$.

2*H*-2,3-Dihydro-3-bromo-1,5-benzodioxepin (7), A solution of 1.0 g (0.006 mol) of 2*H*-2,3-dihydro-3-hydroxy-1,5-benzodioxepin in 100 mL of anhydrous dichloromethane and 2.14 g (0.012 mol) of *N*-bromosuccinide was cooled to 0 °C. Afterwards, 3.16 g (0.012 mol) of triphenylphosphine in 30 mL of dichloromethane was added dropwise, and the mixture as stirred 48 h at room temperature. The dichloromethane was then evaporated, and the product was purified by flash chromatography on silica gel, by using 50:50 hexane/dichloromethane as eluent giving 1.1 g (80%) of a colorless liquid: ^1H NMR δ ($CDCl_3$) 3.97–4.66 (5 H, m, CH_2O + CH), 6.96 (4 H, s, Ar); mass spectrum calcd for $C_9H_9O_2Br$, M 277.9786, found (70 eV) 277.9782 $(M)^+$, 149 $(M-Br)^+$, 121 $(M-Br-CH-CH_2)^+$.

2*H*-2,3-Dihydro-3-iodo-1,5-benzodioxepin (8), A mixture of 1.4 g (0.0057 mol) of 2*H*-2,3-dihydro-3-mesylate-1,5-benzodioxepin, 4.2 g (0.028 mol) of NaI, and 50 mL of isobutylene methyl ketone was refluxed for 16 h. The solution was then cooled to room temperature, and the solvent was evaporated under reduced pressure. The product was purified by flash chromatography on silica gel by using 70% hexane and 30% dichloromethane as eluent giving 1.069 g (68%) of a brown solid. This product was sublimated at 45 °C under reduced pressure giving a white solid: mp = 60 °C; ^1H NMR δ ($CDCl_3$) 4.00–4.70 (5 H, m, CH_2–O + CH) 6.96 (4 H, s, Ar); mass spectrum calcd for $C_9H_9O_2I$, M 275.9606, found (70 eV) 275.9643 $(M)^+$, 149 $(M-I)^+$, 121 $(M-I-CH-CH_2)^+$.

Acknowledgment. We acknowledge the assistance of Dr. Phan Viet Minh Tan, manager of the "Laboratoire Régional de RMN à Haut Champ" in Montréal. We thank the Natural Sciences and Engineering Research Council of Canda for financial support.

Supplementary Material Available: Figures depicting the ^1H and ^{13}C spectra for compounds **5**, **7**, and **8** at variable temperatures together with detailed spectral analysis (11 pages). Ordering information is given on any current masthead page.

(26) Inagaki, S.; Iwase, K.; Mori, Y. *Chem. Lett.* **1986**, 417.
(27) Christian, G. D. *Analytical Chemistry*; 3rd ed.; John Wiley & Sons: New York, 1980.